# Theory of two-photon induced fluorescence anisotropy decay in membranes

Sun-Yung Chen and B. Wieb Van Der Meer
Department of Physics and Astronomy, Western Kentucky University, Bowling Green, Kentucky 42101 USA

ABSTRACT We report the first theoretical description for the time-dependent fluorescence anisotropy decay resulted from two-photon excitation ($r_{[2]}(t)$) for fluorophores in macroscopically isotropic and oriented membranes. In case of two-photon excitation, the initial value of the fluorescence anisotropy $r_{[2]}(0)$ immediately after excitation by a flash of polarized light is a function of the components of the two-photon absorption transition tensor $\underline{\underline{S}}$ and the projections of the emission transition moment to the principal axes of $\underline{\underline{S}}$. The components of $\underline{\underline{S}}$ depend on the symmetries of all molecular states relevant to the two-photon absorption process. The maximal value of $r_{[2]}(0)$ is proven to be as large as 0.61 in contrast to 0.4 for the conventional one-photon induced fluorescence anisotropy $r_{[1]}(0)$. It is shown that only for some special cases the ratio of the two-photon $r_{[2]}(t)$ over the conventional one-photon $r_{[1]}(t)$ will be a constant at all times for fluorophores in macroscopically isotropic membrane systems. In oriented membrane systems, an additional order parameter $\langle P_6 \rangle$ can be determined by the use of angle-resolved fluorescence depolarization measurements resulted from two-photon excitation. The advantages of measuring time-resolved fluorescence anisotropy decays or angle-resolved fluorescence depolarization ratios by two-photon excitation for the study of orientational dynamics in isotropic or oriented membranes are discussed from the theoretical point of view.

## INTRODUCTION

The application of two-photon excitation to the field of biophysics has been of considerable interest just recently. Instead of using the conventional ultraviolet light, the same excited singlet state of the fluorophore can be populated by using a longer and less damaging wavelength of excitation source (e.g., the red light) via the two-photon absorption process. In comparison with the one-photon excitation cross section, the two-photon excitation cross section for a typical molecule is extremely low at the intensity of conventional light sources. With the help of ultrafast pulsed lasers, a very high local instantaneous intensity can be achieved at the point where the laser beam is focused. Using the quadratic intensity dependence of two-photon excitation and using a pulsed laser, fluorescence from two-photon excitation was shown to enhance the signal-to-background ratio and spatial resolution of fluorescence imaging in laser scanning microscopy without using confocal spatial filters and ultraviolet optics (1, 2).

The two-photon absorption probability depends not only on intensity but also on the polarizations of those two exciting photons. By the use of polarized two-photon absorption studies, the symmetries of all excited molecular states involved in the two-photon process can be elucidated (3–6). Moreover, the two-photon induced fluorescence depolarizations of fluorophores in various solvents and at different temperatures have been studied by frequency-domain fluorometry (7, 8). A significantly higher limiting fluorescence anisotropy $r(0)$ was reported by using two-photon excitation than by one-photon excitation in these studies. The observed higher limiting anisotropy value indicates that a higher oriented population was photoselected by two-photon excitation. Two-photon excitation was therefore suggested to be able to enhance the experimental resolution for time-resolved fluorescence anisotropy measurements (7, 8). To justify the above experimental finding and the suggested advantage of applying two-photon excitation to time-resolved fluorescence anisotropy measurements, we have developed a theory of time-dependent fluorescence anisotropy in membranes upon two-photon excitation. The application of two-photon excitation to angle-resolved fluorescence depolarization measurements is also shown to provide more information on the equilibrium orientational distribution of fluorophores in oriented membrane systems.

## THEORY OF TWO-PHOTON INDUCED FLUORESCENCE ANISOTROPY DECAY

### In macroscopically isotropic membranes

We begin with defining the two-photon experimental setup as follows: let ($X_L$, $Y_L$, $Z_L$) be the laboratory coordinate system and the fluorescent sample be placed at the origin. Linearly polarized light travels along the $X_L$ axis with polarization along the $\underline{Z}_L$ direction and excites the sample. In this case all exciting photons are polarized in the direction of $\underline{Z}_L$, a unit vector along the $Z_L$ axis. The fluorescence emission intensity polarized along the $\underline{Z}_L$ direction (vertical), $I_V$, and along the $\underline{X}_L$ direction (horizontal), $I_H$, are observed along the $Y_L$ axis. Here $\underline{X}_L$ is a unit vector along the $X_L$ axis. On the basis of the above experimental condition, the time-dependent fluorescence anisotropy can then be defined as

$$r(t) = (I_V - I_H)/(I_V + 2I_H). \quad (1)$$

Address correspondence to Dr. S. Chen.


0006-3495/93/05/1567/09 $2.00

Because of the involvement of intermediate states during the two-photon absorption process, the photoselection rule for two-photon absorption is much more complicated than that for one-photon absorption. In general, the polarization dependence of two-photon absorption probability is proportional to $(\underline{\mu}\cdot\underline{\underline{S}}\cdot\underline{\lambda})^2$ (3), where $\underline{\mu}$ and $\underline{\lambda}$ are unit vectors representing polarizations of those two incident photons, and $\underline{\underline{S}}$ is a Cartesian tensor of second rank and denoting the two-photon absorption transition tensor in a molecule-fixed coordinate system. The $\alpha\beta$th element of the Cartesian tensor $\underline{\underline{S}}$ is defined as (3–5):

$$S_{\alpha\beta} = \sum_n \left[\frac{\langle g|\alpha|n\rangle\langle n|\beta|f\rangle + \langle g|\beta|n\rangle\langle n|\alpha|f\rangle}{E_n - h\nu}\right], \quad (2)$$

where $|g\rangle$ and $|f\rangle$ are the ground state and the final excited state, respectively. These two molecular states are connected via simultaneous two-photon absorption of the incident frequency $\nu$. $E_n$ is the energy of the virtual intermediate state $|n\rangle$. In this article two identical exciting photons are considered such that both $\underline{\mu}$ and $\underline{\lambda}$ are equal to $\underline{Z}_L$. The tensor elements of $\underline{\underline{S}}$ depend on the symmetries of all the relevant transition states of the fluorophore during the two-photon absorption process. For identical photon experiments, the two-photon transition tensors will be symmetric (i.e., $S_{\alpha\beta} = S_{\beta\alpha}$) as can be seen from Eq. 2.

The probabilities of fluorescence emission along the $Z_L$ and $X_L$ axes are proportional to $(\underline{e}\cdot\underline{Z}_L)^2$ and $(\underline{e}\cdot\underline{X}_L)^2$, respectively. Here $\underline{e}$, a unit vector, denotes the direction of the emission transition moment and $(\underline{e}\cdot\underline{Z}_L)$ and $(\underline{e}\cdot\underline{X}_L)$ are projections of the emission transition moment on the $Z_L$ and $X_L$ axes, respectively. Since the emitted intensity is proportional to the ensemble average of the product of the probability that the fluorophore is excited at time 0 (two-photon absorption) and the probability that the fluorophore is emitted at time $t$, $I_V$ and $I_H$ can be described as follows:

$$I_V = K\langle(\underline{Z}_L\cdot\underline{\underline{S}}_0\cdot\underline{Z}_L)^2(\underline{e}_t\cdot\underline{Z}_L)^2\rangle, \quad (3)$$

$$I_H = K\langle(\underline{Z}_L\cdot\underline{\underline{S}}_0\cdot\underline{Z}_L)^2(\underline{e}_t\cdot\underline{X}_L)^2\rangle. \quad (4)$$

Where $K$ is dependent on the fluorescence intensity decay law of the fluorophore and also proportional to absorbance and concentration of fluorophores in the sample; $\underline{\underline{S}}_0$ and $\underline{e}_t$ represent the two-photon absorption transition tensor at time 0 and the emission transition moment at time $t$, respectively. The brackets denote the ensemble average over all molecular orientations of fluorophores in the sample up to time $t$.

For liquids, vesicles, or membrane suspensions, any chosen local coordinate system of the membrane can be considered to be spherically distributed with respect to the laboratory coordinate system since the sample is macroscopically isotropic. Here the local coordinate system is a Cartesian coordinate system that is either molecule-fixed or having its z-axis along the membrane normal. On averaging over all possible orientations for the local coordinate system with respect to the laboratory coordinate system, the time-dependent fluorescence anisotropy function upon two-photon excitation, $r_{[2]}(t)$, can be evaluated.

In an isotropic system, cylindrical symmetry about the laboratory $Z_L$ axis ensures that $I_H$ can be written as

$$\begin{aligned} I_H &= K\langle(\underline{Z}_L\cdot\underline{\underline{S}}_0\cdot\underline{Z}_L)^2(\underline{e}_t\cdot\underline{X}_L)^2\rangle \\ &= K\langle(\underline{Z}_L\cdot\underline{\underline{S}}_0\cdot\underline{Z}_L)^2(\underline{e}_t\cdot\underline{Y}_L)^2\rangle \\ &= \frac{K}{2}\langle(\underline{Z}_L\cdot\underline{\underline{S}}_0\cdot\underline{Z}_L)^2[1-(\underline{e}_t\cdot\underline{Z}_L)^2]\rangle. \end{aligned} \quad (5)$$

Combining Eqs. 3 and 5 yields

$$\begin{aligned} I_V + 2I_H &= K\langle(\underline{Z}_L\cdot\underline{\underline{S}}_0\cdot\underline{Z}_L)^2\rangle \\ &= K\left\langle\left[\sum_{\alpha,\beta=x,y,z} S_{\alpha\beta}(0)(\underline{\alpha}\cdot\underline{Z}_L)(\underline{\beta}\cdot\underline{Z}_L)\right]^2\right\rangle, \end{aligned} \quad (6)$$

and

$$\begin{aligned} I_V - I_H &= K\langle(\underline{Z}_L\cdot\underline{\underline{S}}_0\cdot\underline{Z}_L)^2P_2(\underline{e}_t\cdot\underline{Z}_L)\rangle \\ &= K\left\langle\left[\sum_{\alpha,\beta=x,y,z} S_{\alpha\beta}(0)(\underline{\alpha}\cdot\underline{Z}_L)(\underline{\beta}\cdot\underline{Z}_L)\right]^2\right. \\ &\quad \left.\times P_2(\underline{e}_t\cdot\underline{Z}_L)\right\rangle. \end{aligned} \quad (7)$$

Here $S_{\alpha\beta}(0)$ is the $\alpha\beta$th element of the Cartesian tensor $\underline{\underline{S}}_0$ in a local coordinate system (x, y, z) at time 0; $P_2$ is the 2nd rank Legendre polynomial and $P_2(\underline{e}_t\cdot\underline{Z}_L) = {}^3/_2(\underline{e}_t\cdot\underline{Z}_L)^2 - {}^1/_2$; $\underline{\alpha}$ and $\underline{\beta}$ are unit vectors and run over three coordinate directions $\underline{x}$, $\underline{y}$, and $\underline{z}$.

The orientations of $\underline{e}_t$ and $\underline{Z}_L$ can be denoted by the polar ($\theta$) and azimuthal ($\varphi$) angles with respect to the (x, y, z) coordinates. It is important to realize that the ensemble averages involve integrating over all polar and azimuthal angles weighted with a distribution function of the time $t$. It is advantageous to evaluate the integration over the polar and azimuthal angles of $\underline{Z}_L$ first for all the terms containing the projections of $\underline{Z}_L$ to the x, y, or z axes. On performing this time-independent ensemble averaging for $\underline{Z}_L$, Eqs. 6 and 7 become (see Appendix):

$$I_V + 2I_H = \frac{1}{15}K[2(\underline{\underline{S}}:\underline{\underline{S}}) + (tr\underline{\underline{S}})^2], \quad (8)$$

$$\begin{aligned} I_V - I_H = \frac{2}{35}K(tr\underline{\underline{S}})\langle\underline{e}_t\cdot\underline{\underline{S}}_0\cdot\underline{e}_t\rangle + \frac{4}{35}K\langle\underline{e}_t\cdot\underline{\underline{S}}_0\cdot\underline{\underline{S}}_0\cdot\underline{e}_t\rangle \\ - \frac{2}{105}K[2(\underline{\underline{S}}:\underline{\underline{S}}) + (tr\underline{\underline{S}})^2]. \end{aligned} \quad (9)$$

Here we use the following definitions:

$$tr\underline{\underline{S}} = \sum_\alpha S_{\alpha\alpha} = S_{xx} + S_{yy} + S_{zz}, \quad (10)$$

$$\underline{\underline{S}}:\underline{\underline{S}} = \sum_{\alpha,\beta} S_{\alpha\beta}S_{\beta\alpha}, \quad (11)$$

$$\underline{e}_t\cdot\underline{\underline{S}}_0\cdot\underline{e}_t = \sum_{\alpha,\beta} e_\alpha(t)S_{\alpha\beta}(0)e_\beta(t), \quad (12)$$

$$\underline{e}_t \cdot \underline{\underline{S}}_0 \cdot \underline{\underline{S}}_0 \cdot \underline{e}_t = \sum_{\alpha,\beta,\gamma} e_\alpha(t) S_{\alpha\beta}(0) S_{\beta\gamma}(0) e_\gamma(t), \quad (13)$$

here all subscripts ($\alpha$, $\beta$, and $\gamma$) run over x, y, and z. Both $tr\underline{\underline{S}}$ and $\underline{\underline{S}}:\underline{\underline{S}}$ are invariants (independent of coordinates and time) because the two-photon tensor $\underline{\underline{S}}$ is symmetric ($S_{\alpha\beta} = S_{\beta\alpha}$) for identical photon experiments. The above results can also be obtained from McClain's (4) general derivation for the special case of two identical photons. If the principal axes of $\underline{\underline{S}}$ are chosen as the coordinates and they are perpendicular to each other, then Eqs. 8 and 9 can be further simplified to

$$I_V + 2I_H = \frac{1}{15} K[2(S_{xx}^2 + S_{yy}^2 + S_{zz}^2) + (tr\underline{\underline{S}})^2], \quad (14)$$

$$I_V - I_H = \frac{4}{105} K \sum_{\alpha} S_{\alpha\alpha}(2S_{\alpha\alpha} + tr\underline{\underline{S}}) \langle P_2(\underline{\alpha} \cdot \underline{e}_t) \rangle, \quad (15)$$

here $S_{\alpha\alpha}$ is the diagonal element of $\underline{\underline{S}}$ ($S_{xx}$, $S_{yy}$, $S_{zz}$), and $\underline{\alpha}$ sums over $\underline{x}$, $\underline{y}$, and $\underline{z}$. Eq. 15 can be reduced to only two terms by the use of the following property (see Appendix for proof).

$$\langle P_2(\underline{x} \cdot \underline{e}_t) \rangle + \langle P_2(\underline{y} \cdot \underline{e}_t) \rangle + \langle P_2(\underline{z} \cdot \underline{e}_t) \rangle = 0. \quad (16)$$

Upon substituting $\langle P_2(\underline{x} \cdot \underline{e}_t) \rangle$ for $-(\langle P_2(\underline{y} \cdot \underline{e}_t) \rangle + \langle P_2(\underline{z} \cdot \underline{e}_t) \rangle)$, Eq. 15 becomes:

$$\begin{aligned} I_V - I_H = {} & \frac{4}{105} K[S_{yy}(2S_{yy} + tr\underline{\underline{S}}) - S_{xx}(2S_{xx} + tr\underline{\underline{S}})] \\ & \times \langle P_2(\underline{y} \cdot \underline{e}_t) \rangle \\ & + \frac{4}{105} K[S_{zz}(2S_{zz} + tr\underline{\underline{S}}) - S_{xx}(2S_{xx} + tr\underline{\underline{S}})] \\ & \times \langle P_2(\underline{z} \cdot \underline{e}_t) \rangle. \end{aligned} \quad (17)$$

Usually a fluorescent probe with cylindrical symmetry is used for studying the static and dynamic properties of membranes. If the two-photon transition tensor of the probe under study has the property of $S_{xx} \approx S_{yy}$, Eq. 17 then becomes:

$$\begin{aligned} I_V - I_H = {} & \frac{4}{105} K[S_{zz}(2S_{zz} + tr\underline{\underline{S}}) - S_{xx}(2S_{xx} + tr\underline{\underline{S}})] \\ & \times \langle P_2(\underline{z} \cdot \underline{e}_t) \rangle. \end{aligned} \quad (18)$$

Combining Eqs. 14 and 18, we obtain

$$r_{[2]}(t) = \frac{4}{7} M \langle P_2(\underline{z} \cdot \underline{e}_t) \rangle, \quad (19)$$

and

$$M = \frac{S_{zz}(2S_{zz} + tr\underline{\underline{S}}) - S_{xx}(2S_{xx} + tr\underline{\underline{S}})}{2(2S_{xx}^2 + S_{zz}^2) + (tr\underline{\underline{S}})^2}. \quad (20)$$

From the computer simulation a maximal value of 1.0716 can be obtained for $M$ (e.g., when $S_{xx} = S_{yy} = -0.12$ and $S_{zz} = 0.92$). In this case the initial fluorescence anisotropy $r_{[2]}(0)$ can be as large as 0.61 when the emission transition dipole is along the molecular z axis.

In the case of $|S_{zz}| \gg |S_{xx}| \approx |S_{yy}|$, the value of $M$ will be approximately equal to one and

$$r_{[2]}(t) \approx \frac{4}{7} \langle P_2(\underline{z} \cdot \underline{e}_t) \rangle. \quad (21)$$

Interestingly, the above expression of $r_{[2]}(t)$ is similar to that of the conventional one-photon $r_{[1]}(t)$, which reads

$$r_{[1]}(t) = \frac{2}{5} \langle P_2(\underline{a}_0 \cdot \underline{e}_t) \rangle, \quad (22)$$

where $\underline{a}_0$ is a unit vector along the direction of the absorption transition moment at time 0 (9, 10). If the one-photon transition moment $\underline{a}_0$ of the probe is roughly along the molecular long axis (the z-axis), then $r_{[2]}(t)$ and $r_{[1]}(t)$ will have the similar time-dependent decay behavior. In this case the final function form of $r_{[2]}(t)$ will be like that of $r_{[1]}(t)$, which depends on the packing symmetry of the membrane and the rotational modes of the probe in the membrane (11). Note that a constant ratio of 10:7 ($\approx$1.43) can be obtained for $r_{[2]}(t)/r_{[1]}(t)$ only in this special case. On the contrary, if a probe with $|S_{zz}| \ll |S_{xx}| \approx |S_{yy}|$ is used in the fluorescence experiment, then $M$ will be approximately equal to $-1/2$ and therefore

$$r_{[2]}(t) \approx -\frac{2}{7} \langle P_2(\underline{z} \cdot \underline{e}_t) \rangle. \quad (23)$$

In this case a range of $-5/7$ ($\approx -0.71$) to $10/7$ ($\approx$1.43) is possible for the ratio of $r_{[2]}/r_{[1]}$ depending on the direction of one-photon absorption transition moment.

## In macroscopically oriented membranes

A propagating light wave in a uniaxial medium such as an oriented membrane can have two independent directions of polarizations of the electric field (12). The first, the ordinary ray, has its electric field polarized perpendicular to the axis of symmetry for all angles of incidence. The second, extraordinary ray, is polarized in the plane of incidence, that is, the plane through the incoming beam and the normal to the oriented membrane. We will assume that the oriented membrane consists of a number of bilayers parallel to each other and to the cover slides (13). The preferred orientation of the molecules in such samples coincides with the normal to the cover slides. In fluorescence depolarization experiments in oriented membranes, it is thus possible to measure the intensity for four combinations of polarized directions: $I_{oo}$, $I_{oe}$, $I_{eo}$, and $I_{ee}$. Here the suffix o denotes the ordinary ray and the suffix e denotes the extraordinary ray: the first suffix refers to the exciting light and the second corresponds to the emitted light (12). To eliminate the dependence of these intensities on unknown quantities, such as the incident light intensity and illuminated volume, the depolarization ratios $R_o = I_{oe}/I_{oo}$ and $R_e =$

$I_{eo}/I_{ee}$ are measured. The experimental arrangements for measuring these ratios are depicted in Fig. 1. Other geometries are also possible (14). The unit vector $\underline{\mathbf{p}}$ and $\underline{\mathbf{r}}$ denote the extraordinary polarization directions of the emitted and incident light, respectively, and are defined as:

$$\underline{\mathbf{p}} = \underline{z}\cos\theta + \underline{y}\sin\theta, \tag{24}$$

$$\underline{\mathbf{r}} = \underline{z}\cos\phi + \underline{y}\sin\phi. \tag{25}$$

The depolarization ratios for the two-photon fluorescence are given by

$$R_{o[2]} = \langle(\underline{x}\cdot\underline{\underline{S}}\cdot\underline{x})^2(\underline{\mathbf{e}}_t\cdot\underline{\mathbf{p}})^2\rangle/\langle(\underline{x}\cdot\underline{\underline{S}}\cdot\underline{x})^2(\underline{\mathbf{e}}_t\cdot\underline{x})^2\rangle, \tag{26}$$

$$R_{e[2]} = \langle(\underline{\mathbf{r}}\cdot\underline{\underline{S}}\cdot\underline{\mathbf{r}})^2(\underline{\mathbf{e}}_t\cdot\underline{x})^2\rangle/\langle(\underline{\mathbf{r}}\cdot\underline{\underline{S}}\cdot\underline{\mathbf{r}})^2(\underline{\mathbf{e}}_t\cdot\underline{\mathbf{p}})^2\rangle. \tag{27}$$

It is of interest to consider the special case where the only dominant principal axis of the tensor $\underline{\underline{S}}$ is along the molecular direction $\underline{\mathbf{a}}_0$ and the emission moment is also along $\underline{\mathbf{a}}_0$, which is a unit vector. At time 0, immediately after excitation by a flash of polarized light, the depolarization ratio $R_{o[2]}$ in this case is:

$$R_{o[2]}(0) = \frac{\cos^2\theta\langle(\underline{x}\cdot\underline{\mathbf{a}}_0)^4(\underline{z}\cdot\underline{\mathbf{a}}_0)^2\rangle + \sin^2\theta\langle(\underline{x}\cdot\underline{\mathbf{a}}_0)^4(\underline{y}\cdot\underline{\mathbf{a}}_0)^2\rangle}{\langle(\underline{x}\cdot\underline{\mathbf{a}}_0)^6\rangle}. \tag{28}$$

Here we make use of the fact that due to symmetry the average of $(\underline{x}\cdot\underline{\mathbf{a}}_0)^4(\underline{z}\cdot\underline{\mathbf{a}}_0)(\underline{y}\cdot\underline{\mathbf{a}}_0)$ vanishes. The ratio $R_{e[2]}(0)$ can be calculated similarly. Because of azimuthal symmetry around the z-axis, the averages $\langle(\underline{x}\cdot\underline{\mathbf{a}}_0)^4(\underline{z}\cdot\underline{\mathbf{a}}_0)^2\rangle$, $\langle(\underline{x}\cdot\underline{\mathbf{a}}_0)^4(\underline{y}\cdot\underline{\mathbf{a}}_0)^2\rangle$, and $\langle(\underline{x}\cdot\underline{\mathbf{a}}_0)^6\rangle$ can be reduced to:

$$\langle(\underline{x}\cdot\underline{\mathbf{a}}_0)^4(\underline{z}\cdot\underline{\mathbf{a}}_0)^2\rangle = \frac{3}{8}\langle(1-\xi^2)^2\xi^2\rangle, \tag{29}$$

$$\langle(\underline{x}\cdot\underline{\mathbf{a}}_0)^4(\underline{y}\cdot\underline{\mathbf{a}}_0)^2\rangle = \frac{1}{16}\langle(1-\xi^2)^3\rangle, \tag{30}$$

$$\langle(\underline{x}\cdot\underline{\mathbf{a}}_0)^6\rangle = \frac{5}{16}\langle(1-\xi^2)^3\rangle, \tag{31}$$

where $\xi$ denotes $\underline{\mathbf{a}}_0\cdot\underline{z}$. $R_{o[2]}(0)$ can be rewritten as:

$$R_{o[2]}(0) = \frac{1}{5}[A_2 - (A_2 - 1)\sin^2\theta] \tag{32}$$

with

$$A_2 = \frac{6\langle(1-\xi^2)^2\xi^2\rangle}{\langle(1-\xi^2)^3\rangle}. \tag{33}$$

Using the order parameter $\langle P_2\rangle$, $\langle P_4\rangle$, and $\langle P_6\rangle$ defined as:

$$\langle P_2\rangle = \left\langle\frac{3}{2}\xi^2 - \frac{1}{2}\right\rangle, \tag{34}$$

$$\langle P_4\rangle = \left\langle\frac{35}{8}\xi^4 - \frac{30}{8}\xi^2 + \frac{3}{8}\right\rangle, \tag{35}$$

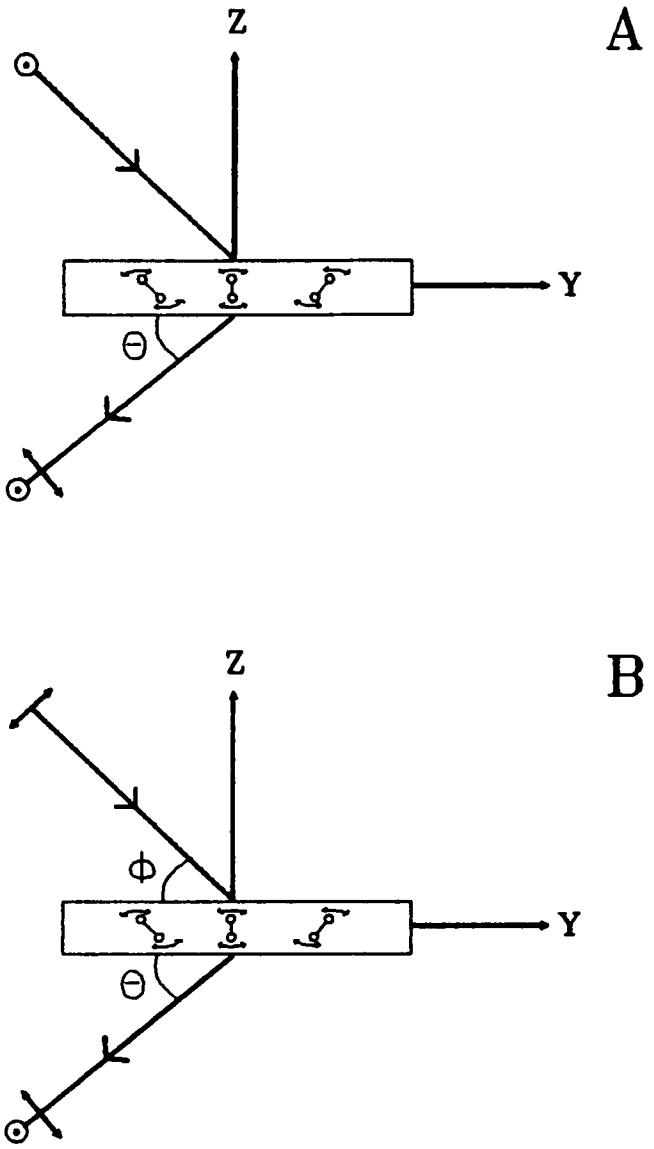


FIGURE 1 (*A*) Experimental arrangement for measuring the "ordinary ratio," $R_o = I_{oe}/I_{oo}$, $I_{oe}$ is the intensity of the fluorescence at excitation with polarized light in the ordinary direction (the *X*-axis, perpendicular to the page) viewed through a polarizer in the extraordinary direction (in the *Z Y*-plane, perpendicular to the fluorescent beam), and $I_{oo}$ the fluorescence intensity for which both excitation and emission polarizers are along the *X*-axis. The angle $\theta$ between the fluorescent beam and the plane of the membrane can be varied. (*B*) Experimental arrangement for measuring the "extraordinary ratio," $R_e = I_{eo}/I_{ee}$, $I_{eo}$ is the intensity of the fluorescence at excitation with polarized light in the extraordinary direction (in the *Z Y*-plane, perpendicular to the incident beam) viewed through a polarizer along the *X*-direction, $I_{ee}$ is the intensity for which both excitation and emission polarizers are along the extraordinary direction. In the incident beam, the polarization is in the *Z Y*-plane perpendicular to the incident beam, the polarizer on the emission side is also in the *Z Y*-plane, but perpendicular to the fluorescence beam. Both the angle $\phi$ (between the incident beam and the plane of the membrane) and the angle $\theta$ (between the fluorescent beam and the plane of membrane) can be varied. The preferred direction of the molecules (depicted as dumbbells) is along the *Z*-axis. The system will have some disorder, however, allowing the molecules to undergo wobbling of their long axes (depicted with double arrows) and other motions.

$$\langle P_6 \rangle = \left\langle \frac{231}{16}\xi^6 - \frac{315}{16}\xi^4 + \frac{105}{16}\xi^2 - \frac{5}{16} \right\rangle \quad (36)$$

the parameter $A_2$ can be expressed as

$$A_2 = \frac{3[11 - 21\langle P_4 \rangle + 10\langle P_6 \rangle]}{[33 - 55\langle P_2 \rangle + 27\langle P_4 \rangle - 5\langle P_6 \rangle]}. \quad (37)$$

Note that in one-photon induced fluorescence depolarization the ratio in this case would read (14):

$$R_{o[1]}(0) = \frac{1}{3}[A_1 - (A_1 - 1)\sin^2\theta], \quad (38)$$

with

$$A_1 = \frac{4\langle(1-\xi^2)\xi^2\rangle}{\langle(1-\xi^2)^2\rangle} = \frac{7 + 5\langle P_2 \rangle - 12\langle P_4 \rangle}{7 - 10\langle P_2 \rangle + 3\langle P_4 \rangle}. \quad (39)$$

For a given distribution function the order parameters $\langle P_2 \rangle$, $\langle P_4 \rangle$, and $\langle P_6 \rangle$ are defined as:

$$\langle P_n \rangle = \int_{-1}^{1} P_n(\xi) f(\xi)\, d\xi \quad n = 2, 4, 6, \quad (40)$$

where $\xi = \cos\theta$ ($\theta$ = angle between $\underline{a}_0$ and membrane normal), $f(\xi)$ is the orientational distribution function (equilibrium distribution function), and $P_n(\xi)$ ($n = 2, 4, 6$) are the 2nd, 4th, and 6th order Legendre polynomials. A geometrical interpretation of the possible ranges for these order parameters can be derived as follows: every continuous distribution function can be approximated by a series of delta functions:

$$f(\xi) = \sum_{n=1}^{N} \alpha_n \delta(\xi - \xi_n), \quad (41)$$

where the coefficients $\alpha_n$ are positive or zero and the sum of $\alpha_n$ (from $n = 1$ to $n = N$) is equal to 1, and the values $\xi_n$ are between $-1$ and 1. This approximation becomes better for larger values of the integer $N$. The points $\xi_n$ correspond to points $(x_n, y_n, z_n) = (P_2(\xi_n), P_4(\xi_n), P_6(\xi_n))$ in three-dimensional space forming a polyhedron touching the curve $(P_2(\xi), P_4(\xi), P_6(\xi))$. Parametric three-dimensional plots of the curve $(P_2(\xi), P_4(\xi), P_6(\xi))$ with $0 \le \xi \le 1$ are shown in Fig. 2 from two different viewpoints. The possible values for $\langle P_2 \rangle$, $\langle P_4 \rangle$, and $\langle P_6 \rangle$ correspond to points $(\langle P_2 \rangle, \langle P_4 \rangle, \langle P_6 \rangle)$ inside or at the surface of such polyhedrons. From visual inspection of the $(P_2(\xi), P_4(\xi), P_6(\xi))$ curve, it is clear that these polyhedrons are between the following two surfaces:

$$\text{upper surface} \begin{pmatrix} x \\ y \\ z \end{pmatrix} = (1-\lambda)\begin{pmatrix} 1 \\ 1 \\ 1 \end{pmatrix} + \lambda \begin{pmatrix} P_2(\xi) \\ P_4(\xi) \\ P_6(\xi) \end{pmatrix}, \quad (42)$$

with $0 \le \lambda \le 1$ and $-1 \le \xi \le 1$; and

$$\text{lower surface} \begin{pmatrix} x \\ y \\ z \end{pmatrix} = (1-\mu)\begin{pmatrix} -1/2 \\ 3/8 \\ -5/16 \end{pmatrix} + \mu \begin{pmatrix} P_2(\xi) \\ P_4(\xi) \\ P_6(\xi) \end{pmatrix}, \quad (43)$$

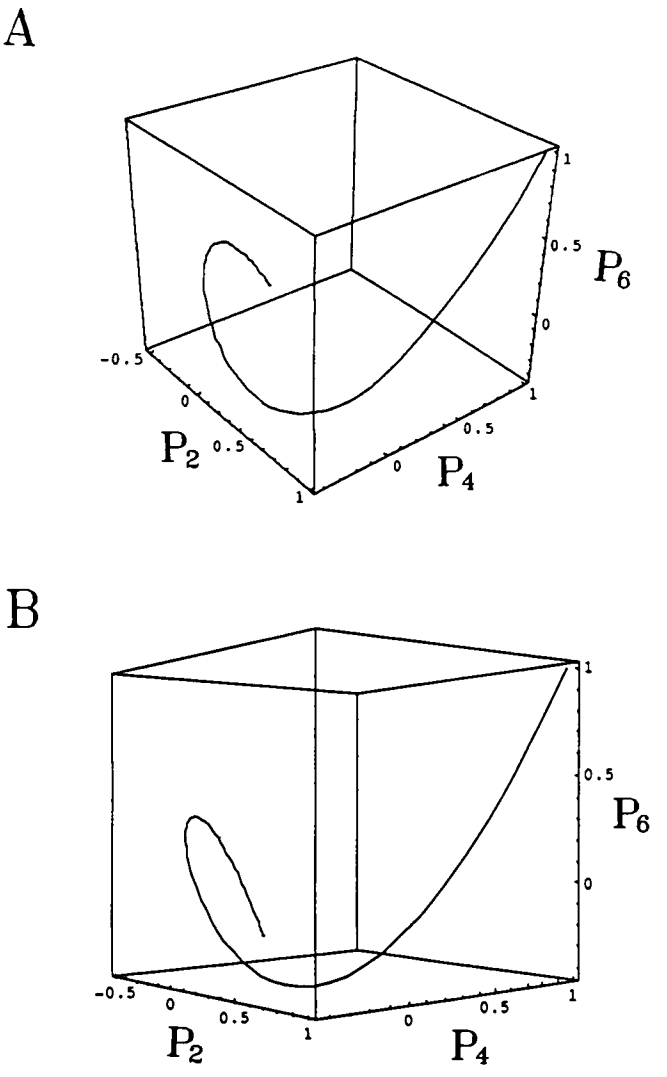


FIGURE 2 The three-dimensional parametric plots of the curve $(P_2(\xi), P_4(\xi), P_6(\xi))$ for $0 \le \xi \le 1$ ($A$) from the viewpoint of (2.64, −2.11, 2) and ($B$) from the viewpoint of (2.64, −2.11, 0). These plots are made by using the Mathematica program.

with $0 \le \mu \le 1$ and $-1 \le \xi \le 1$. This geometrical relation yields an inequality for $\langle P_6 \rangle$ at given $\langle P_2 \rangle$ and $\langle P_4 \rangle$:

$$-\frac{5}{16}(1-\mu) + \mu P_6(\xi) \le \langle P_6 \rangle \le 1 - \lambda + \lambda P_6(\xi_2), \quad (44)$$

where $\lambda$, $\mu$, $\xi_1$, and $\xi_2$ are given by

$$\langle P_2 \rangle = 1 - \lambda + \lambda P_2(\xi_2) = -\frac{1}{2}(1-\mu) + \mu P_2(\xi_1), \quad (45)$$

$$\langle P_4 \rangle = 1 - \lambda + \lambda P_4(\xi_2) = \frac{3}{8}(1-\mu) + \mu P_4(\xi_1). \quad (46)$$

Solving for $\lambda$, $\mu$, $\xi_1$, and $\xi_2$ and expressing $\lambda$, $\mu$, $P_2(\xi_1)$, $P_2(\xi_2)$, $P_4(\xi_1)$, and $P_4(\xi_2)$ in terms of $\langle P_2 \rangle$ and $\langle P_4 \rangle$

and substituting these expressions back into the inequality (44) yields:

$$-\frac{5}{16}+\frac{35}{352}\left(\langle P_2\rangle+\frac{1}{2}\right)G \le \langle P_6\rangle \le 1-\frac{49}{88}(1-\langle P_2\rangle)H, \quad (47)$$

$$G=\frac{1}{5}\left[\frac{27}{7}+\frac{264}{35}\left(\frac{\langle P_4\rangle-{}^3/_8}{\langle P_2\rangle+{}^1/_2}\right)\right]^2-1, \quad (48)$$

$$H=\frac{1}{7}\left[-\frac{25}{7}+\frac{132}{35}\left(\frac{1-\langle P_2\rangle}{1-\langle P_4\rangle}\right)\right]^2+1. \quad (49)$$

The range of possible values of $\langle P_6\rangle$ for given $\langle P_2\rangle$ and $\langle P_4\rangle$ can be estimated by using the above inequality. For instance, if $\langle P_2\rangle = 0.6$ and $\langle P_4\rangle = 0.5$, then the range of possible $\langle P_6\rangle$ values will be from 0.064 to 0.736. Fig. 3 shows the values of $R_{o[1]}(0)$ and $R_{o[2]}(0)$ as a function of $\sin^2\theta$ ($\theta$ is the angle between the fluorescent beam and the plane of the membrane) for an oriented membrane system with $\langle P_2\rangle = 0.6$ and $\langle P_4\rangle = 0.5$. A wide range of $R_{o[2]}(0)$ is possible for this given pair of order parameters. The lower and upper limits of $R_{o[2]}(0)$ are shown in Fig. 3 and they correspond to the $\langle P_6\rangle$ value of 0.064 and 0.736, respectively.

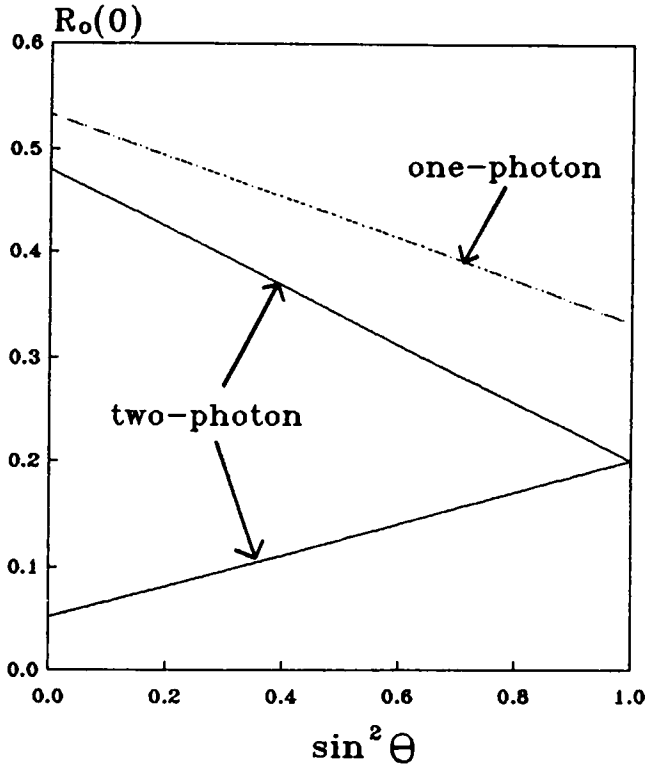


FIGURE 3 A plot of the limiting depolarization ratio $R_o(0)$ with the ordinary ray incident as a function of $\sin^2\theta$ ($\theta$ is the angle between the fluorescent beam and the plane of the membrane) by one-photon excitation $R_{o[1]}(0)$ (*dotted line*) and two-photon excitation $R_{o[2]}(0)$ (*solid line*). The dotted line is drawn for a system with $\langle P_2\rangle = 0.6$ and $\langle P_4\rangle = 0.5$. The upper solid line is drawn for a system with $\langle P_2\rangle = 0.6$, $\langle P_4\rangle = 0.5$, and $\langle P_6\rangle = 0.736$ (the maximum value for $\langle P_6\rangle$ in this case). The lower solid line is for a system with $\langle P_2\rangle = 0.6$, $\langle P_4\rangle = 0.5$, and $\langle P_6\rangle = 0.064$ (the minimum value for $\langle P_6\rangle$ in the case).

## DISCUSSION

From frequency-domain fluorescence anisotropy measurements, a constant anisotropy ratio ($r_{[2]}/r_{[1]}$) of $1.44 \pm 0.02$ ($\approx 10{:}7$) was observed for both 2,5-diphenyloxazole (PPO) in propylene glycol (7) and 1,6-diphenylhexatriene (DPH) in triacetin (8) at all frequencies. This corresponds to a constant ratio of $r_{[2]}(t)/r_{[1]}(t)$ at all times. Because of this identical time-dependent decay behavior of one- and two-photon $r(t)$, it appears to signify that the two-photon transition tensor of both PPO and DPH possesses a dominant element and the corresponding axis is along the one-photon transition moment. However, the reported $r_{[2]}(0)$ values of PPO and DPH are 0.54 and 0.52, respectively (7, 8). These values are significantly smaller than the predicted $r_{[2]}(0)$ value of 0.57 for molecules with $|S_{zz}| \gg |S_{xx}| \approx |S_{yy}|$. These lower $r_{[2]}(0)$ values imply that the emission dipole is not exactly along the dominant axis of $\underline{\underline{S}}$ or $S_{zz}$ is not completely dominant among all $\underline{\underline{S}}$ components. Moreover, the suggested advantage of the higher $r(0)$ value resulted from two-photon excitation for the resolution of fluorescence anisotropy measurement will be canceled out by the weaker signal resulted from two-photon excitation compared with one-photon excitation.

Note that the general two-photon induced time-dependent fluorescence anisotropy decay is very complicated and depends not only on the patterns of $\underline{\underline{S}}$ but also on the time-dependent correlations of $\underline{e}_t$ to all three principal axes of $\underline{\underline{S}}$ at time 0 (see Eqs. 8 and 9). Even for a planar molecule like anthracene with $D_{2h}$ symmetry, the photon-selection probability for the two-photon $B_{1g} \leftarrow A_{1g}$ transition is proportional to $(\cos\Theta \sin\Theta \cos\beta)^2$ (15) and not simply to $\cos^4\Theta$, which was used for those elongated fluorophores (7, 8). Here $\Theta$ is the angle between a chosen molecular axis and the excitation polarization and $\beta$ is the angle between the plane of the molecule and the plane perpendicular to the excitation polarization (15). In this case the ratio of two-photon fluorescence anisotropy over one-photon fluorescence anisotropy can be proven to be 5:14 (instead of 10:7), which will cause a decrease (instead of an increase) for the resolution of time-resolved fluorescence anisotropy decay measurements. Ideally, only when the two-photon transition tensor of the probe satisfies the special conditions discussed in the theory section, theoretical dynamic models and their corresponding functional forms of $r_{[1]}(t)$ in liquids (16), and macroscopically isotropic membrane systems (9–11) can still be applied to the two-photon case by simply multiplying with a constant. Note that the two-photon experiments we have mentioned here were using two identical photons. If two photons of mixed polarizations are used to investigate the system, a different time-dependent fluorescence anisotropy decay profile can be

expected due to a different photon-selection process. The information concerning the two-photon induced excited state symmetry and the rotational dynamics of the fluorophore with respect to each of its molecular axes could be resolved by the use of a combination of mixed polarized photons.

The application of two-photon excitation to angle-resolved fluorescence depolarization measurements has been demonstrated to provide a more precise picture about the equilibrium orientational distribution of fluorophores in an oriented membrane system. The limiting value of $R_{o[2]}$ at time 0 obtained from angle-resolved fluorescence anisotropy measurements can be used to extract the value of the sixth rank order parameter, $\langle P_6 \rangle$, which was considered to be inaccessible by the conventional one-photon induced fluorescence measurements (10–12). In combination with the second and fourth rank order parameters ($\langle P_2 \rangle$ and $\langle P_4 \rangle$) obtained from conventional one-photon induced angle-resolved fluorescence measurements, a more detailed molecular orientational distribution for the membrane system can be reconstructed.

In summary, two-photon excitation can complicate the time-dependent fluorescence anisotropy decay behavior of fluorophores in membranes due to the depolarization effects from all transition moments involved in the two-photon process. However, if fluorophores with special two-photon transition tensors are used, the time-dependent fluorescence anisotropy decay in isotropic membranes by two-photon excitation and that by one-photon excitation will have a constant ratio with respect to each other at all times. In this case, two-photon excitation can be further utilized to provide more detailed orientational distribution information for the fluorophore in oriented membranes by angle-resolved fluorescence depolarization measurements. Otherwise the two-photon transition tensor of a specific fluorophore needs to be evaluated first by differential absorption studies of linearly and circularly polarized light of fluorophores in isotropic solution. Then the corresponding time-dependent fluorescence anisotropy decay behavior of that fluorophore in membranes can be derived.

## APPENDIX

In macroscopically isotropic membrane systems, molecules are isotropically distributed with respect to the laboratory coordinate system. Consider the term $\langle (\underline{\alpha} \cdot \underline{Z}_L)(\underline{\beta} \cdot \underline{Z}_L)(\underline{\gamma} \cdot \underline{Z}_L)(\underline{\rho} \cdot \underline{Z}_L) \rangle$, where $\underline{\alpha}$, $\underline{\beta}$, $\underline{\gamma}$, or $\underline{\rho}$ equals $\underline{x}$, $\underline{y}$, or $\underline{z}$, which are unit vectors along the local x-, y-, and z-axis, respectively. Note that in this term at least two of the four unit vectors ($\underline{\alpha}$, $\underline{\beta}$, $\underline{\gamma}$, $\underline{\rho}$) must be equal to each other. For evaluating this term, a new local coordinate system is defined with the z′-axis along this pair of identical unit vectors, the x′-axis perpendicular to the z′-axis, and the y′-axis perpendicular to both the z′- and x′-axis, with the unit vectors $\underline{x}'$, $\underline{y}'$, and $\underline{z}'$, along the x′-, y′-, and z′-axis, respectively. Using this new coordinate system, it is found that $\langle (\underline{\alpha} \cdot \underline{Z}_L)(\underline{\beta} \cdot \underline{Z}_L)(\underline{\gamma} \cdot \underline{Z}_L)(\underline{\rho} \cdot \underline{Z}_L) \rangle$ can have three possible values:

1. $$\langle (\underline{\alpha} \cdot \underline{Z}_L)(\underline{\beta} \cdot \underline{Z}_L)(\underline{\gamma} \cdot \underline{Z}_L)(\underline{\rho} \cdot \underline{Z}_L) \rangle = \frac{1}{4\pi} \int_0^{2\pi} \int_0^{\pi} \cos^4\theta \sin\theta \, d\theta \, d\varphi = \frac{1}{5} \quad \text{if} \quad \alpha = \beta = \gamma = \rho.$$

2. $$\langle (\underline{\alpha} \cdot \underline{Z}_L)(\underline{\beta} \cdot \underline{Z}_L)(\underline{\gamma} \cdot \underline{Z}_L)(\underline{\rho} \cdot \underline{Z}_L) \rangle = \frac{1}{4\pi} \int_0^{2\pi} \int_0^{\pi} \cos^2\theta \sin^2\theta \cos^2\varphi \sin\theta \, d\theta \, d\varphi$$
$$= \frac{1}{4\pi} \int_0^{2\pi} \int_0^{\pi} \cos^2\theta \sin^2\theta \sin^2\varphi \sin\theta \, d\theta \, d\varphi = \frac{1}{15}$$
if $(\alpha = \beta \neq \gamma = \rho) \vee (\alpha = \gamma \neq \beta = \rho) \vee (\alpha = \rho \neq \beta = \gamma)$.

3. $$\langle (\underline{\alpha} \cdot \underline{Z}_L)(\underline{\beta} \cdot \underline{Z}_L)(\underline{\gamma} \cdot \underline{Z}_L)(\underline{\rho} \cdot \underline{Z}_L) \rangle = \frac{1}{4\pi} \int_0^{2\pi} \int_0^{\pi} \cos^3\theta \sin\theta \cos\varphi \sin\theta \, d\theta \, d\varphi$$
$$= \frac{1}{4\pi} \int_0^{2\pi} \int_0^{\pi} \cos^3\theta \sin\theta \sin\varphi \sin\theta \, d\theta \, d\varphi$$
$$= \frac{1}{4\pi} \int_0^{2\pi} \int_0^{\pi} \cos^2\theta \sin^2\theta \sin\varphi \cos\varphi \sin\theta \, d\theta \, d\varphi = 0$$
for all other cases.

These three results can be summarized in one equation, using the Kronecker delta, $\delta_{ij}$, $\delta_{ij} = 1$ if $i = j$, and $\delta_{ij} = 0$, if $i \neq j$ ($i, j = \alpha, \beta, \gamma$, or $\rho$):

$$\langle (\underline{\alpha} \cdot \underline{Z}_L)(\underline{\beta} \cdot \underline{Z}_L)(\underline{\gamma} \cdot \underline{Z}_L)(\underline{\rho} \cdot \underline{Z}_L) \rangle = \frac{1}{15} (\delta_{\alpha\beta}\delta_{\gamma\rho} + \delta_{\alpha\gamma}\delta_{\beta\rho} + \delta_{\alpha\rho}\delta_{\beta\gamma}). \quad \text{(A1)}$$

Using similar arguments, we find

$$\begin{aligned}\langle (\underline{\alpha} \cdot \underline{Z}_L)(\underline{\beta} \cdot \underline{Z}_L)(\underline{\gamma} \cdot \underline{Z}_L)(\underline{\rho} \cdot \underline{Z}_L)(\underline{\eta} \cdot \underline{Z}_L)(\underline{\psi} \cdot \underline{Z}_L) \rangle &= \frac{1}{105} (\delta_{\alpha\beta}\delta_{\gamma\rho}\delta_{\eta\psi} + \delta_{\alpha\beta}\delta_{\gamma\eta}\delta_{\rho\psi} + \delta_{\alpha\beta}\delta_{\gamma\psi}\delta_{\rho\eta} + \delta_{\alpha\gamma}\delta_{\beta\rho}\delta_{\eta\psi} \\ &+ \delta_{\alpha\gamma}\delta_{\beta\eta}\delta_{\rho\psi} + \delta_{\alpha\gamma}\delta_{\beta\psi}\delta_{\rho\eta} + \delta_{\alpha\rho}\delta_{\beta\gamma}\delta_{\eta\psi} + \delta_{\alpha\rho}\delta_{\beta\eta}\delta_{\gamma\psi} \\ &+ \delta_{\alpha\rho}\delta_{\beta\psi}\delta_{\gamma\eta} + \delta_{\alpha\eta}\delta_{\beta\gamma}\delta_{\rho\psi} + \delta_{\alpha\eta}\delta_{\beta\rho}\delta_{\gamma\psi} + \delta_{\alpha\eta}\delta_{\beta\psi}\delta_{\gamma\rho} \\ &+ \delta_{\alpha\psi}\delta_{\beta\gamma}\delta_{\rho\eta} + \delta_{\alpha\psi}\delta_{\beta\rho}\delta_{\eta\gamma} + \delta_{\alpha\psi}\delta_{\beta\eta}\delta_{\gamma\rho}), \end{aligned} \quad \text{(A2)}$$

with $\alpha, \beta, \gamma, \rho, \eta, \psi = x, y, z$.

By using the property of Eq. A1, the ensemble average of $(\underline{Z}_L \cdot \underline{\underline{S}} \cdot \underline{Z}_L)^2$ in Eq. 6 can be evaluated as follows:

$$\begin{aligned}\left\langle \left[ \sum_{\alpha,\beta} S_{\alpha\beta}(0)(\underline{\alpha} \cdot \underline{Z}_L)(\underline{\beta} \cdot \underline{Z}_L) \right]^2 \right\rangle &= \left\langle \sum_{\alpha,\beta,\gamma,\rho} S_{\alpha\beta}(0) S_{\gamma\rho}(0)(\underline{\alpha} \cdot \underline{Z}_L)(\underline{\beta} \cdot \underline{Z}_L)(\underline{\gamma} \cdot \underline{Z}_L)(\underline{\rho} \cdot \underline{Z}_L) \right\rangle \\ &= \frac{1}{15} \sum_{\alpha,\beta,\gamma,\rho} \langle S_{\alpha\beta}(0) S_{\gamma\rho}(0) \rangle (\delta_{\alpha\beta}\delta_{\gamma\rho} + \delta_{\alpha\gamma}\delta_{\beta\rho} + \delta_{\alpha\rho}\delta_{\beta\gamma}) \\ &= \frac{1}{15} \sum_{\alpha,\gamma} \langle S_{\alpha\alpha}(0) S_{\gamma\gamma}(0) \rangle + \frac{1}{15} \sum_{\alpha,\beta} \langle S_{\alpha\beta}(0) S_{\alpha\beta}(0) \rangle \\ &+ \frac{1}{15} \sum_{\alpha,\beta} \langle S_{\alpha\beta}(0) S_{\beta\alpha}(0) \rangle. \end{aligned} \quad \text{(A3)}$$

On further using the definitions of $tr\underline{\underline{S}}$ and $\underline{\underline{S}}:\underline{\underline{S}}$ (see Eqs. 10 and 11), we arrive at

$$\left\langle \left[ \sum_{\alpha,\beta} S_{\alpha\beta}(0)(\underline{\alpha} \cdot \underline{Z}_L)(\underline{\beta} \cdot \underline{Z}_L) \right]^2 \right\rangle = \frac{1}{15} (tr\underline{\underline{S}})^2 + \frac{2}{15} \underline{\underline{S}}:\underline{\underline{S}}. \quad \text{(A4)}$$

Note that these terms are independent of time (see text). Similarly, the ensemble average in Eq. 7 can be evaluated using Eqs. A2. It is demonstrated as follows:

$$\left\langle \left[ \sum_{\alpha,\beta} S_{\alpha\beta}(0)(\underline{\alpha}\cdot\underline{Z}_L)(\underline{\beta}\cdot\underline{Z}_L) \right]^2 P_2(\underline{e}_t\cdot\underline{Z}_L) \right\rangle$$

$$= \frac{3}{2} \sum_{\alpha,\beta,\gamma,\rho,\eta,\psi} \langle S_{\alpha\beta}(0)S_{\gamma\rho}(0)(\underline{e}_t\cdot\underline{\eta})(\underline{e}_t\cdot\underline{\psi})(\underline{\alpha}\cdot\underline{Z}_L)(\underline{\beta}\cdot\underline{Z}_L)(\underline{\gamma}\cdot\underline{Z}_L)(\underline{\rho}\cdot\underline{Z}_L)(\underline{\eta}\cdot\underline{Z}_L)(\underline{\psi}\cdot\underline{Z}_L)\rangle$$

$$- \frac{1}{2} \left\langle \left[ \sum_{\alpha,\beta} S_{\alpha\beta}(0)(\underline{\alpha}\cdot\underline{Z}_L)(\underline{\beta}\cdot\underline{Z}_L) \right]^2 \right\rangle$$

$$= \frac{1}{70} \sum_{\alpha,\beta,\gamma,\rho,\eta,\psi} \langle S_{\alpha\beta}(0)S_{\gamma\rho}(0)(\underline{e}_t\cdot\eta)(\underline{e}_t\cdot\psi)\rangle (\delta_{\alpha\rho}\delta_{\gamma\beta}\delta_{\eta\psi} + \delta_{\alpha\rho}\delta_{\gamma\eta}\delta_{\beta\psi} + \delta_{\alpha\rho}\delta_{\gamma\psi}\delta_{\beta\eta} + \delta_{\alpha\gamma}\delta_{\beta\rho}\delta_{\eta\psi} + \delta_{\alpha\gamma}\delta_{\beta\eta}\delta_{\rho\psi} + \delta_{\alpha\gamma}\delta_{\beta\psi}\delta_{\eta\rho} + \delta_{\alpha\beta}\delta_{\gamma\rho}\delta_{\eta\psi}$$

$$+ \delta_{\alpha\beta}\delta_{\gamma\eta}\delta_{\rho\psi} + \delta_{\alpha\beta}\delta_{\gamma\psi}\delta_{\eta\rho} + \delta_{\alpha\eta}\delta_{\gamma\rho}\delta_{\psi\beta} + \delta_{\alpha\eta}\delta_{\gamma\psi}\delta_{\beta\rho} + \delta_{\alpha\eta}\delta_{\gamma\beta}\delta_{\rho\psi} + \delta_{\alpha\psi}\delta_{\gamma\rho}\delta_{\eta\beta} + \delta_{\alpha\psi}\delta_{\gamma\eta}\delta_{\beta\rho} + \delta_{\alpha\psi}\delta_{\gamma\beta}\delta_{\eta\rho}) - \frac{1}{30}(tr\underline{\underline{S}})^2 - \frac{1}{15}\underline{\underline{S}}:\underline{\underline{S}}$$

$$= \frac{1}{70}\Bigg[ \sum_{\alpha,\gamma} S_{\alpha\alpha}(0)S_{\gamma\gamma}(0) + \sum_{\alpha\gamma\rho} S_{\alpha\alpha}(0)S_{\gamma\rho}(0)(\underline{e}_t\cdot\underline{\rho})(\underline{e}_t\cdot\underline{\gamma}) + \sum_{\alpha\gamma\rho} S_{\alpha\alpha}(0)S_{\gamma\rho}(0)(\underline{e}_t\cdot\underline{\gamma})(\underline{e}_t\cdot\underline{\rho}) + \sum_{\alpha\beta} S_{\alpha\beta}(0)S_{\alpha\beta}(0)$$

$$+ \sum_{\alpha\beta\rho} S_{\alpha\beta}(0)S_{\alpha\rho}(0)(\underline{e}_t\cdot\underline{\beta})(\underline{e}\cdot\underline{\rho}) + \sum_{\alpha\beta\rho} S_{\alpha\beta}(0)S_{\alpha\rho}(0)(\underline{e}_t\cdot\underline{\beta})(\underline{e}_t\cdot\underline{\rho}) + \sum_{\alpha\beta} S_{\alpha\beta}(0)S_{\beta\alpha}(0)$$

$$+ \sum_{\alpha\beta\gamma} S_{\alpha\beta}(0)S_{\gamma\alpha}(0)(\underline{e}_t\cdot\underline{\beta})(\underline{e}_t\cdot\underline{\gamma}) + \sum_{\alpha\beta\gamma} S_{\alpha\beta}(0)S_{\gamma\alpha}(0)(\underline{e}_t\cdot\underline{\beta})(\underline{e}_t\cdot\underline{\gamma}) + \sum_{\alpha\beta\gamma} S_{\alpha\beta}(0)S_{\gamma\gamma}(0)(\underline{e}_t\cdot\underline{\alpha})(\underline{e}_t\cdot\underline{\beta})$$

$$+ \sum_{\alpha\beta\gamma} S_{\alpha\beta}(0)(\underline{e}_t\cdot\alpha)(\underline{e}_t\cdot\gamma) + \sum_{\alpha\beta\gamma} S_{\alpha\beta}(0)S_{\gamma\gamma}(0)(\underline{e}_t\cdot\underline{\beta})(\underline{e}_t\cdot\underline{\alpha}) + \sum_{\alpha\beta\gamma} S_{\alpha\beta}(0)S_{\gamma\beta}(0)(\underline{e}_t\cdot\underline{\alpha})(\underline{e}_t\cdot\underline{\gamma})$$

$$+ \sum_{\alpha\beta\rho} S_{\alpha\beta}(0)S_{\beta\rho}(0)(\underline{e}_t\cdot\underline{\alpha})(\underline{e}_t\cdot\underline{\rho}) + \sum_{\alpha\beta\rho} S_{\alpha\beta}(0)S_{\beta\rho}(0)(\underline{e}_t\cdot\underline{\alpha})(\underline{e}_t\cdot\underline{\rho})\Bigg] - \frac{1}{30}(tr\underline{\underline{S}})^2 - \frac{1}{15}\underline{\underline{S}}:\underline{\underline{S}}. \qquad \text{(A5)}$$

By using the definitions 10–13, a more compact final expression can be obtained as follows:

$$\left\langle \left[ \sum_{\alpha,\beta} S_{\alpha\beta}(0)(\underline{\alpha}\cdot\underline{Z}_L)(\underline{\beta}\cdot\underline{Z}_L) \right]^2 P_2(\underline{e}_t\cdot\underline{Z}_L) \right\rangle$$

$$= \frac{2}{35} trS\langle \underline{e}_t\cdot\underline{\underline{S}}_0\cdot\underline{e}_t\rangle + \frac{4}{35}\langle \underline{e}_t\cdot\underline{\underline{S}}_0\cdot\underline{\underline{S}}_0\cdot\underline{e}_t\rangle$$

$$- \frac{4}{105}\underline{\underline{S}}:\underline{\underline{S}} - \frac{2}{105}(tr\underline{\underline{S}})^2 \qquad \text{(A6)}$$

Eq. 16 in the theory section can be proven as follows:

$$\langle P_2(\underline{x}\cdot\underline{Z}_L)\rangle + \langle P_2(\underline{y}\cdot\underline{Z}_L)\rangle + \langle P_2(\underline{z}\cdot\underline{Z}_L)\rangle$$

$$= \langle P_2(\underline{x}\cdot\underline{Z}_L) + P_2(\underline{y}\cdot\underline{Z}_L) + P_2(\underline{z}\cdot\underline{Z}_L)\rangle$$

$$= \left\langle \frac{3}{2}[(\underline{x}\cdot\underline{Z}_L)^2 + (\underline{y}\cdot\underline{Z}_L)^2 + (\underline{z}\cdot\underline{Z}_L)^2] - \frac{3}{2} \right\rangle$$

$$= \left\langle \frac{3}{2} - \frac{3}{2} \right\rangle = 0 \qquad \text{(A7)}$$

We thank Drs. Barry Brunson and Claus Ernst (Department of Mathematics, Western Kentucky University) for their help with using the Mathematica program. We also thank Dr. P. R. Callis (Department of Chemistry, Montana State University) for his helpful discussions regarding all possible shapes of the two-photon absorption tensor.

This work was supported by a grant from the National Science Foundation (EHR-9108764).

*Received for publication 10 July 1992 and in final form 19 January 1993.*

## REFERENCES

1. Piston, D. W., D. R. Sandison, and W. W. Webb. 1992. Time-resolved fluorescence imaging and background rejection by two-photon excitation in laser scanning microscopy. *SPIE (Soc. Photooptical Instrument. Eng.).* 1640:379–389.
2. Denk, W., J. H. Strickler, and W. W. Webb. 1991. Two-photon excitation in laser scanning microscopy. *Science (Wash. DC).* 248:73–76.
3. McClain, W. M. 1971. Excited state symmetry assignment through polarized two-photon absorption studies of fluids. *J. Chem. Phys.* 55:2789–2796.
4. McClain, W. M. 1972. Polarization dependence of three-photon phenomena for randomly oriented molecules. *J. Chem. Phys.* 57:2264–2272.
5. Scott, T. W., K. S. Haber, and A. C. Albrecht. 1983. Two-photon photoselection in rigid solutions: a study of the $B_{2u} \leftarrow A_{1g}$ transition in benzene. *J. Chem. Phys.* 78:150–157.
6. Cable, J. R., and A. C. Albrecht. 1986. Theory of three-photon photoselection with application to the hexagonal point groups. *J. Chem. Phys.* 85:3145–3154.
7. Lakowicz, J. R., I. Gryczynski, E. Danielsen, and M. J. Wirth. 1992. Time-resolved fluorescence intensity and anisotropy decays of 2,5-diphenyloxazole by two-photon excitation and frequency-domain fluorometry. *J. Phys. Chem.* 96:3000–3006.
8. Lakowicz, J. R., I. Gryczynski, and E. Danielsen. 1992. Anomalous differential polarized phase angles for two-photon excitation with isotropic depolarizing rotations. *Chem. Phys. Lett.* 191:47–53.

9. Szabo, A. 1984. Theory of fluorescence depolarization in macromolecules and membranes. *J. Chem. Phys.* 81:150–167.

10. Van Der Meer, B. W., H. Pottel, W. Herreman, M. Ameloot, H. Hendrickz, and H. Schroder. 1984. Effect of orientational order on the decay of the fluorescence anisotropy in membrane suspensions. *Biophys. J.* 46:515–523.

11. Van Der Meer, B. W., K. H. Cheng, and S.-Y. Chen. 1990. Effects of lateral diffusion on the fluorescence anisotropy in hexagonal lipid phases. I. Theory. *Biophys. J.* 46:515–523.

12. Van Der Meer, B. W., R. P. H. Kooyman, and Y. K. Levine. 1982. A theory of fluorescence depolarization in macroscopically ordered membrane system. *Chem. Phys.* 66:39–50.

13. Kooyman, R. P. H., Y. K. Levine, and B. W. Van Der Meer. 1981. Measurement of 2nd and 4th rank order parameters by fluorescence polarization in a lipid membrane system. *Chem. Phys.* 60:317–326.

14. Vogel, H., and F. Jähnig. 1985. Fast and slow orientational fluctuations in membranes. *Proc. Natl. Acad. Sci. USA.* 82:2029–2033.

15. Peticolas, W. L., R. Norris, and K. E. Rieckhoff. 1965. Polarization effects in the two-photon excitation of anthracene fluorescence. *J. Chem. Phys.* 42:4164–4169.

16. Weber, G. 1952. Polarization of the fluorescence of solutions. *In* Fluorescence and Phosphorescence Analysis. K. M. Hercules, editor. John Wiley and Sons, New York. 217–240.